

Supporting Information

Sulfur vacancy-rich N-doped MoS₂ nanoflower for highly boosting electrocatalytic N₂ fixation to NH₃ under ambient conditions

Libin Zeng,^{a, b} Shuai Chen,^a Joshua van der Zalm,^a Xinyong Li^{*a, b} and Aicheng Chen^{*a}

^a Electrochemical Technology Center, Department of Chemistry, University of Guelph, 50 Stone Road East, Guelph, ON N1G 2W1, Canada

^b State Key Laboratory of Fine Chemicals, Key Laboratory of Industrial Ecology and Environmental Engineering (MOE), School of Environmental Science and Technology, Dalian University of Technology, Dalian 116024, China

Number of pages (including cover page): 24

Number of figures: 8 (figures S1-S9)

Number of tables: 5 (tables S1-S5)

Table of Contents

I.	Experimental Section	S3-S5
II.	Electrochemical Measurements	S5-S6
III.	Characterization	S6
IV.	Theoretical Calculations	S6-S7
V.	NH ₃ Quantification	S7-S8
VI.	Figures	S10-S18
VII.	Tables	S19-S23
VIII.	References	S24

Experimental Section

Chemicals

Sodium molybdate dehydrate ($\text{Na}_2\text{MoO}_4 \cdot 2\text{H}_2\text{O}$), sodium sulfide (Na_2S), ammonium fluoride (NH_4F), Nafion (5 wt%) solution, sodium hydroxide (NaOH), sodium salicylate ($\text{C}_7\text{H}_5\text{O}_3\text{Na}$), sodium hypochlorite (NaClO), sodium nitroferricyanide (III) ($\text{C}_5\text{FeN}_6\text{Na}_2\text{O}$), ammonium chloride (NH_4Cl), and sodium sulfate (Na_2SO_4) were purchased from Sigma-Aldrich Chemical Reagent Co., Ltd. Nitric acid (99.99%), sulfuric acid (99.99%), hydrochloric acid (HCl), and ethanol were purchased from Aladdin Ltd.. All reagents were of analytical grade and used without further purification. A cation exchange membrane (CEM) was purchased from the DuPont Company. All glassware was treated with aqua regia and thoroughly rinsed with Millipore water ($18.2 \text{ M}\Omega \cdot \text{cm}$). Deionized water was used in all experiments.

Fabrication of N@MoS₂ catalyst

The MoS₂ nanoflower synthesis process followed former work with some modifications.¹ As follows: 1 mM $\text{Na}_2\text{MoO}_4 \cdot 2\text{H}_2\text{O}$ was dissolved in 35 mL deionized water, after which 5 mM Na_2S was added into the solution under stirring for 10 min. Subsequently, the mixture was transferred into a 50 mL Teflon-lined autoclave in a muffle furnace maintained at 200°C for 24 h. After cooling to room temperature, the obtained catalyst was rinsed several times with deionized water and ethanol. After drying at 80°C under vacuum

overnight, a pure MoS₂ nanoflower catalyst was obtained. To obtain the N-doped MoS₂ nanoflowers, 100 mg of MoS₂ catalyst with different NH₄F quantities (50, 100, and 200 mg) were mixed and ground, respectively. This powder was placed in a quartz boat and heated to 500°C for 2 h with a heating rate of 10 °C min⁻¹ under argon flow in a tube furnace. The finally obtained samples were designated as N@MoS₂-1, N@MoS₂, and N@MoS₂-2, respectively. For contrast, pure MoS₂ microflowers were treated similarly, without the introduction of NH₄F.

Preparation of working electrodes

The catalyst ink was prepared for electrode fabrication as follows.² Catalyst powder (5 mg) was dispersed in a mixed 960 μL water/ethanol solution (V/V = 1:1). A 40 μL Nafion solution (1 wt%) was then added under continuous sonication for 60 min. The catalyst ink (10 μL) was then introduced dropwise onto a well-polished glassy-carbon electrode (Ø3 mm) and dried at room temperature.

CEM treatment

The CEM was initially oxidized in a 10% H₂O₂ solution at 80 °C for 60 min, and then treated with a 0.5 M H₂SO₄ solution for an additional 60 min. Following several rinses with deionized water, until the pH value was close to 7, the obtained membrane was vacuum dried at 60°C overnight. Finally, the treated CEM was affixed between the anode

and cathode chambers.

Electrochemical Measurements

The electrochemical characterization experiments were conducted in a three-electrode electrochemical workstation (Voltalab Potentiostat PGZ301) with a gas inflow system (20 mL single cell). The prepared electrode samples were used as the working electrode, whereas an Ag/AgCl (1 M KCl), and Pt wire were employed as the reference and counter electrodes, respectively. The potentials were referenced to a reversible hydrogen electrode (RHE), $E_{\text{RHE}} = E_{\text{Ag/AgCl}} + (0.210 + 0.059 \cdot \text{pH}) \text{ V}$. Prior to the electrochemical experiments, the electrolyte solution was poured into high purity argon gas (99.99%) to remove any residual gas. Linear sweep voltammetry (LSV) was conducted in an Ar- and N₂-saturated 0.1 M Na₂SO₄ solution at a scan rate of 10 mV s⁻¹ to obtain the polarization curves, respectively. The current efficiency was calculated using the following equation:

$$\text{Current Efficiency}\% = [(j_{\text{N}_2} - j_{\text{Ar}}) / j_{\text{N}_2}] \times 100\%$$

where j_{N_2} and j_{Ar} were the current densities measured in the N₂-saturated and Ar-saturated condition, respectively. The electrochemical impedance spectroscopy (EIS) was also tested in the frequency range from 10⁻² Hz to 10⁵ Hz in an Ar- and N₂-saturated 0.1 M Na₂SO₄ solution, respectively. For NRR measurements, the H-type 100 mL cell separated by CEM was used to evaluate the NH₃ amount. Before NRR experiments, the 0.1 M Na₂SO₄ electrolyte was pre-saturated with N₂ gas for 30 min. All experiments were carried out at room temperature.

Characterization

SEM images of the prepared samples were obtained at an accelerating voltage of 10 kV using a Hitachi SU 70, equipped with EDS, which was used to characterize the compositions of the samples. The XRD patterns were recorded with a PW1050-3710 diffractometer using a Cu $k\alpha$ ($\lambda = 1.5405 \text{ \AA}$) radiation source to confirm the crystallinity of the prepared nanomaterials. X-ray photoelectron spectra were acquired using a Thermo Scientific K- α XPS spectrometer. A monochromatic Al K α X-ray source was utilized, with a spot area of 400 μm . Charge compensation was provided, and the position of the energy scale was adjusted to place the main C 1s feature (C-C) at 284.6 eV. All data processing was performed using XPS peak software. The specific surface area and pore size distribution were investigated by nitrogen adsorption/desorption isotherms on a Quantachrome instrument (NOVA 4200e, USA). For the conductivity of catalysts analysis, Nano ZS90 size analyzer (ZEN3690, England) was used to measure 5 mg mL⁻¹ samples dispersed in DI water. For surface defects, low-temperature electronic paramagnetic resonance (EPR) was carried out with the N@MoS₂ samples on a Bruker EPR A200- 9.5/12. The NH₃ yield rate was observed at $\lambda_{max} = 665 \text{ nm}$ using UV-Vis spectrophotometer.

Theoretical Calculation

Density functional theory (DFT) calculations and the density of states of N@MoS₂ were performed with the Perdew-Bruke-Ernzerhof (PBE) functional of the generalized gradient

approximation (GGA) using the CASTEP module.³ The unit cell parameters of N@MoS₂ primarily referred to the XRD and XPS data, and the N content was mainly obtained from the XPS data. The 3D triclinic bulk MoS₂ cell (a = 6.320 Å, b = 6.320 Å, c = 12.29 Å, α = β = 90°, γ = 120°) was selected as the doping model. An energy cutoff of 320 eV and k-point set of 2 × 1 × 1 were proposed to perform geometry optimization and electronic structure calculations. To better study the optimal doping for N and MoS₂, the adsorption energy (E) was defined as

$$\Delta E_N = E_{N@MoS_2}^{Total} + E_S - E_{MoS_2}^{Total} - E_N$$

where $E_{N@MoS_2}^{Total}$, $E_{MoS_2}^{Total}$, E_S and E_N are the total energies of N doped MoS₂, MoS₂, the isolated S and N atoms, respectively.

NH₃ Quantification

In the cathode chamber, the NH₃ product was quantitatively measured by the indophenol blue method.⁴ The detailed experimental process was as follows. Firstly, 2 mL of effluent solution was extracted from the reaction chamber. Subsequently, a 2 mL A solution, containing a 0.32 M NaOH solution was combined with 10.0 g salicylic acid, 10.0 g sodium citrate, and a 1 mL B solution composed of 0.05 M NaClO solution. Next, a 200 μL C solution (0.01 g mL⁻¹) was introduced dropwise into the test samples. Following 2 h, the absorption spectra of these solutions were acquired by a UV-vis spectrophotometer under 500-880 nm. The absorbance of the formed NH₃ concentration was estimated at a wavelength of 655 nm. The concentration vs. absorbance curve (**Fig. S5**) was performed

using a standard NH_4Cl solution with a series of concentrations, from 0.0 to $1.0 \mu\text{g mL}^{-1}$ in $0.1 \text{ M Na}_2\text{SO}_4$. The fitting curve ($y = 0.113x + 0.013$, $R^2 = 0.998$) showed a good linear relation of absorbance value with the NH_3 concentrations via three repeated experiments. The NH_3 concentration was then calculated by the fitting curve, and the NH_3 yield rate was calculated as follows:

$$\text{NH}_3 \text{ yield rate} = \frac{C_{[\text{NH}_4^+]}}{m_{\text{cat.}} \times t} \times V$$

where $C_{[\text{NH}_4^]}$ is the obtained NH_3 concentration; V is the volume of the cathodic reaction electrolyte (100 mL); $m_{\text{cat.}}$ is the loaded quantity of catalyst (0.05 mg); and t is the reduction reaction time;

FE was calculated according to the following equation:

$$\text{FE} = \frac{3 \times F \times C_{[\text{NH}_4^+]}}{18 \times Q} \times V$$

where F is the Faraday constant ($96485.3 \text{ C mol}^{-1}$); and Q is the quantity of applied electricity ($Q = I \times t$).

In order to accurately assess the origin of the produced NH_3 , the experiments were repeated three times. The pH of the electrolyte was also measured in the cathodic compartment. After the 15-hours N_2 reduction, the pH was changed from 6.8 to 8.4.

Detection of N_2H_4

The possible generation of N_2H_4 was investigated by the Watt and Chrisp method.^{5,6} At the optimized potential -0.3 V , after two hours of the NRR, 2.0 mL of the electrolyte was taken and mixed with 2.0 mL of the color reagent ($2.0 \text{ g C}_9\text{H}_{11}\text{NO}$ and $0.14 \text{ g Na}_2\text{SO}_4$ dissolved into 100 mL ethanol) at room temperature. The absorbance of the mixture was

measured at 455 nm wavelength. As shown in Fig. S8, no difference was observed between the initial electrolyte and the electrolyte after the two-hour NRR, indicating that no N_2H_4 was formed.

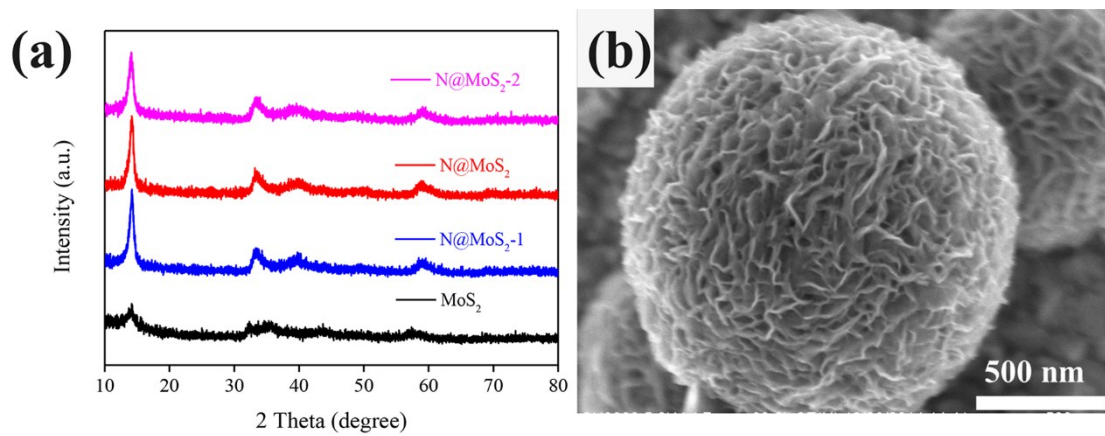


Figure S1. (a) XRD patterns of the as-prepared MoS₂, N@MoS₂-1, N@MoS₂, and N@MoS₂-2 samples; (b) SEM image of the MoS₂ catalyst.

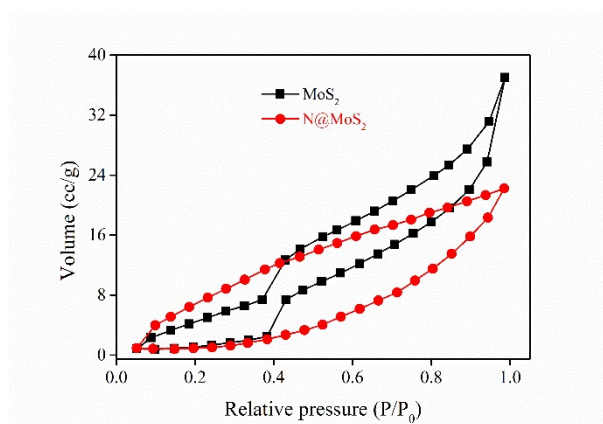


Figure S2. Nitrogen adsorption/desorption isotherms curve of the N doped MoS₂ and MoS₂ samples.

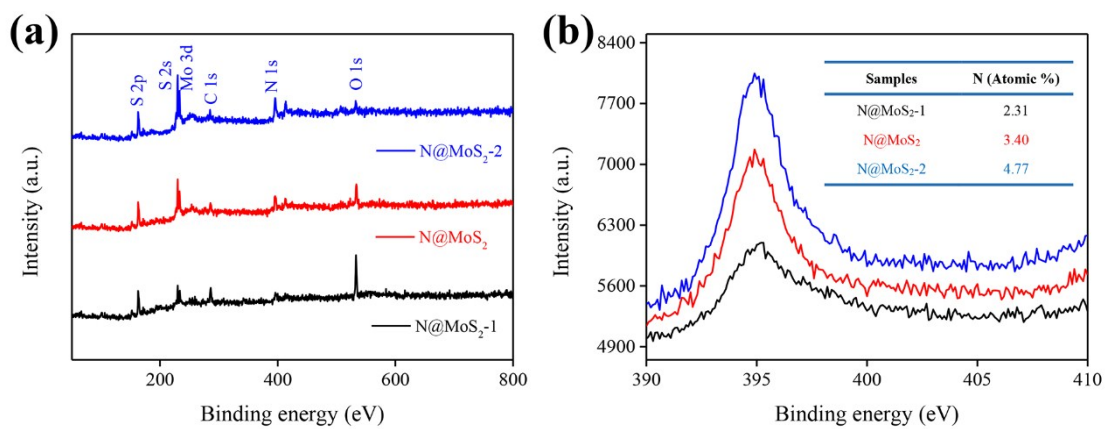


Figure S3. XPS survey spectra of the N@MoS₂ samples, and (b) N 1s high resolution XPS spectra of the as-prepared samples. The inset table is the N content.

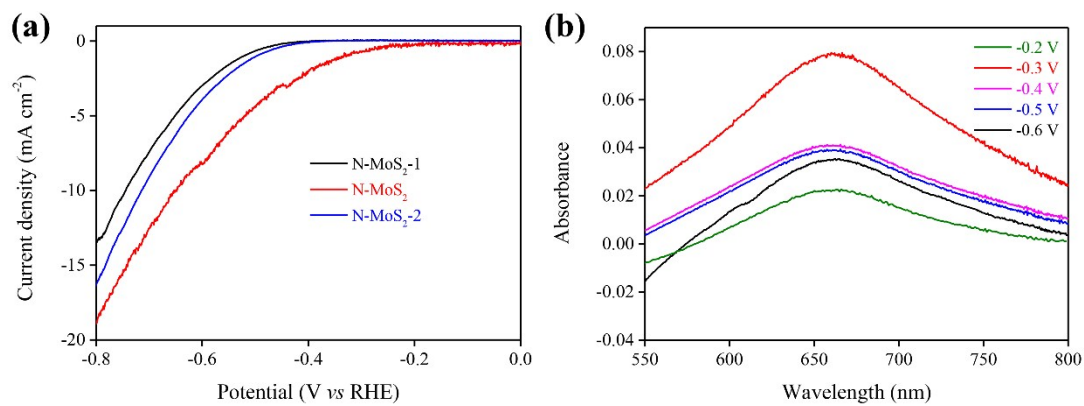


Figure S4. (a) LSV curves of N-doped MoS₂ samples in a N₂-saturated 0.1 M Na₂SO₄ solution, under a scan rate of 10 mV s⁻¹; (b) UV-vis absorption spectra of the electrolytes stained with an indophenol indicator following the NRR reaction under a series of potentials for 2 h.

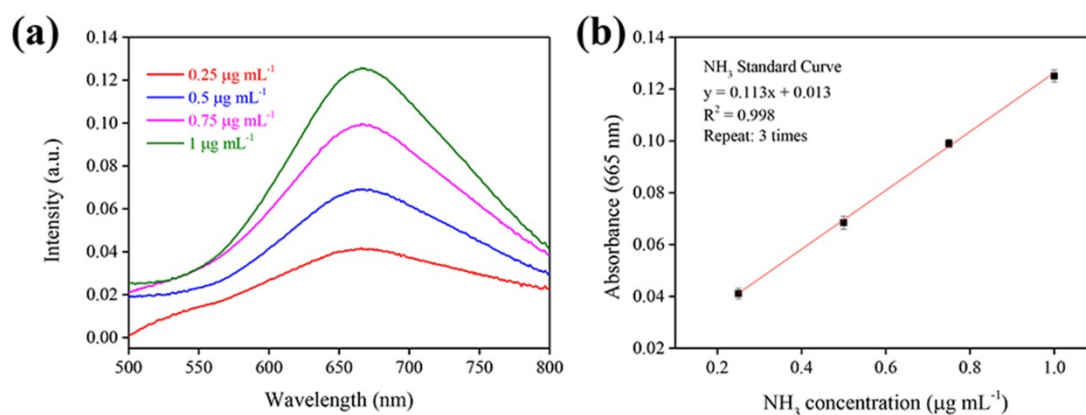


Figure S5. (a) UV-vis curves of the indophenol assays with NH_4^+ ions after incubation for 2 h and (b) calibration curve used for the estimation of NH_3 via NH_4^+ ion concentration.

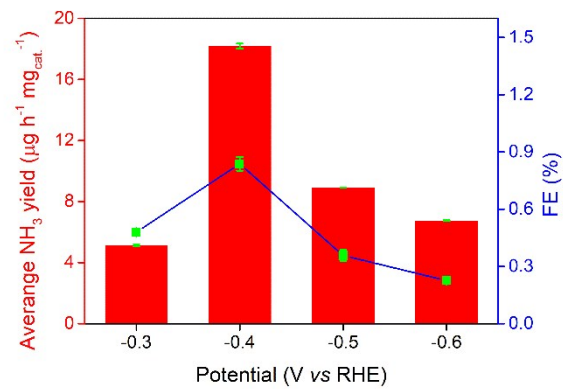


Figure S6. NH₃ yields and corresponding FEs of MoS₂ for NRR at various potentials.

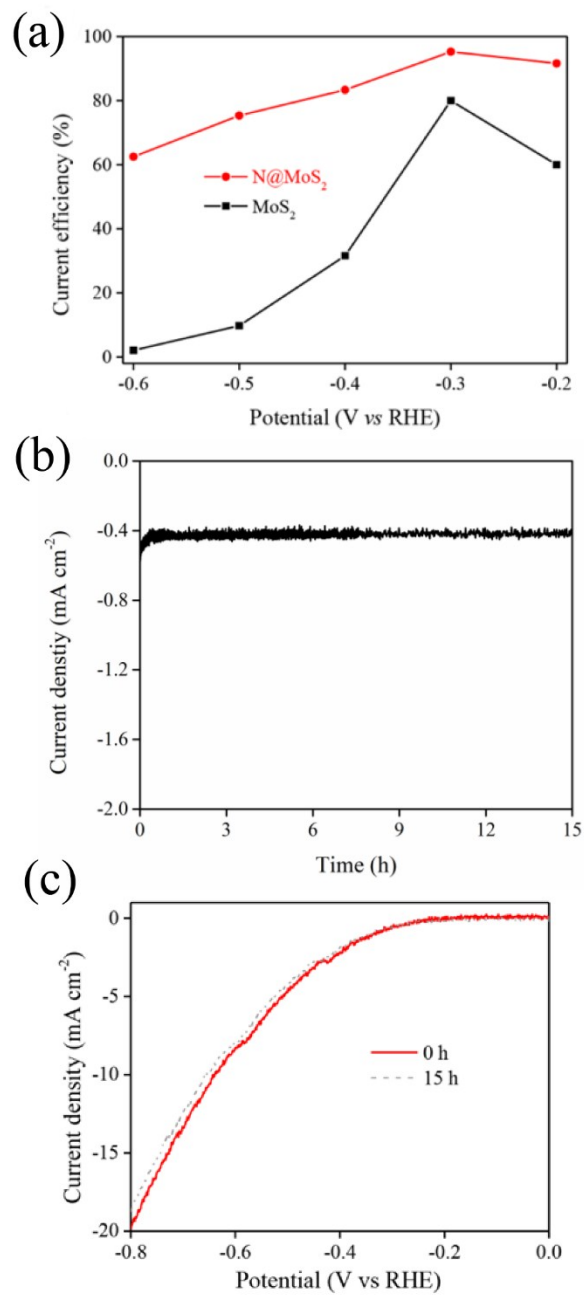


Figure S7. (a) Current efficiency curves of MoS₂ and N@MoS₂ catalysts for the NRR; (b) Current dependent time curve of the N@MoS₂ catalyst at -0.3 V vs. RHE (The curve was performed by a continuous N₂ purging); (c) Comparison of the LSV curves changes in before and after N₂ reduction.

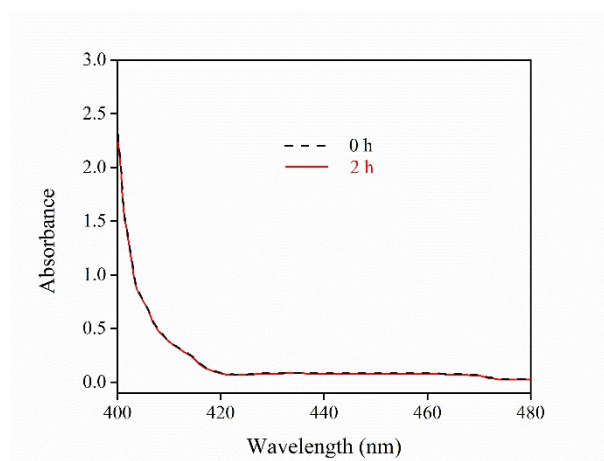


Figure S8. UV-Vis absorption spectra of the electrolytes analyzed for possible N_2H_4 generation during the NRR under N_2 atmosphere at -0.3 V vs RHE.

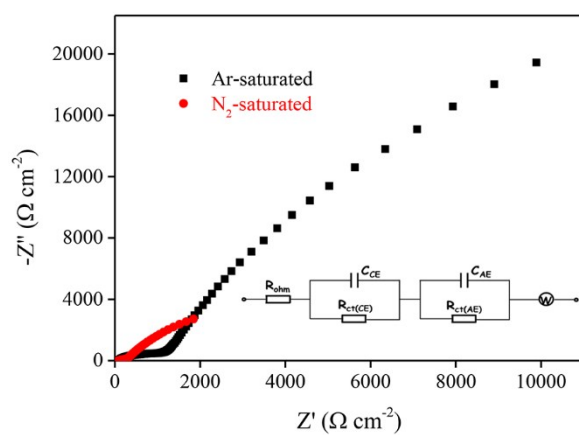


Figure S9. EIS spectra of the N@MoS₂ catalyst at -0.3 V under Ar- and N₂-saturated conditions. Inset: equivalent circuit model.

Table S1. EDX analysis of different N-doped MoS₂ catalysts.

Sample	Mo L (Atomic/%)	S K(Atomic/%)	N K(Atomic/%)
N@MoS ₂ -1	34.24	62.83	2.93
N@MoS ₂	32.70	62.05	5.26
N@MoS ₂ -2	31.32	56.11	12.57

Table S2. Physical properties of the N-doped and single MoS₂ samples.

Sample	Surface areas (m² g⁻¹)	Pore volume (cm³ g⁻¹)	Pore radius (nm)	Conductivity (mS cm⁻²)
MoS ₂	6.26	0.073	3.273	0.010
N@MoS ₂	4.33	0.040	4.559	0.101

Table S3. Comparison of recent studies on electrochemical ammonia synthesis in 0.1 M Na₂SO₄ solution under ambient condition; E: applied potential (V vs. RHE).

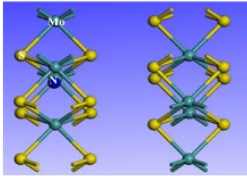
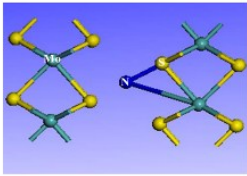
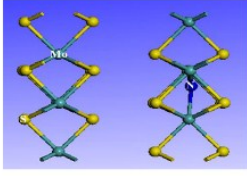
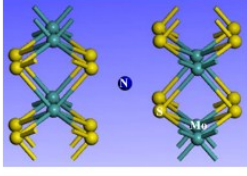
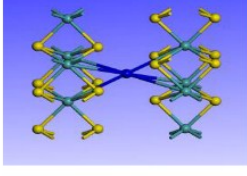
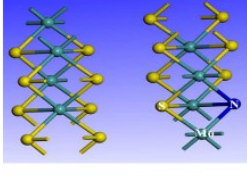
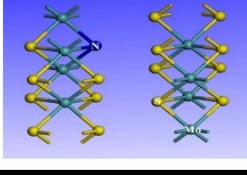
Catalysts	FE (%) /	NH ₃ Yield	Ref.
	E (V)	($\mu\text{g h}^{-1} \text{mg}^{-1}_{\text{cat.}}$) / E (V)	
MoS ₂ nanosheets	1.17/-0.5	13.09/-0.5	7
S-rich MoS ₂ nanoflowers	8.34/-0.4	29.28/-0.4	8
O@C nanosheets	4.67/-0.7	12.39/-0.8	9
S@C nanospheres	7.47/-0.7	19.07/-0.7	10
Mn ₃ O ₄ nanocubes	3.0/-0.8	11.60/-0.8	11
La ₂ O ₃ nanoplates	4.76/-0.8	17.04/-0.8	12
N@MoS ₂ nanoflowers	9.14/-0.3	69.82/-0.3	This work

Table S4. Parameter analysis of the equivalent circuit model corresponding to the Nyquist plots of the as-prepared N-doped MoS₂ under Ar- and N₂-saturated conditions.

Gas-saturated	R _s (Ω cm ²)	C _{CE} (μF cm ²)	R _{ct(CE)} (Ω cm ²)	C _{AE} (mF cm ²)	R _{ct(AE)} (Ω cm ²)	W(S*Sec ⁵ cm ²)
N ₂	6.51 ± 0.07	79.6 ± 0.63	450.7 ± 22.1	10.95 ± 0.01	386.5 ± 7.22	0.01 ± 0
Ar	6.57 ± 0.08	99.8 ± 0.06	(2.53 ± 0.01)*10 ¹⁴	1.3 ± 0	3818 ± 53.4	0.0013 ± 0

R_s = Resistance of solution, R_{ct}(CE) = Charge transfer resistance, R_{ct}(AE) = Charge transfer and recombination resistance, C = Capacitance of double-layer, W = Warburg impedance (mass transfer).

Table S5. Possible N-doped MoS₂ model structures.

Type	Structure
I	
II	
III	
IV	
V	
VI	
VII	

References

1. L. Zeng, X. Li, S. Fan, Z. Yin, M. Zhang, J. Mu, M. Qin, M. Tadé and S. Liu, *Electrochim. Acta*, **2019**, 295, 810-821.
2. X. Y. Yu, Y. Feng, Y. Jeon, B. Guan, X. W. Lou and U. Paik, *Adv. Mater.*, **2016**, 28, 9006-9011.
3. M. Segall, P. J. Lindan, M. a. Probert, C. Pickard, P. J. Hasnip, S. Clark and M. Payne, *J. Phys. Condens. Mat.*, **2002**, 14, 2717-2744.
4. L. Xia, X. Wu, Y. Wang, Z. Niu, Q. Liu, T. Li, X. Shi, A. M. Asiri and X. Sun, *Small Methods*, **2018**, 14, 1800251.
5. D. Zhu, L. Zhang, R. J. Hamers, *Nature Mater.* **2013**, 12, 836-841.
6. J. Christianson, D. Zhu, R. J. Hamers, J. R. Schmidt, *J. Phys. Chem. B* **2014**, 118, 195-203.
7. L. Zhang, X. Ji, X. Ren, Y. Ma, X. Shi, Z. Tian, A. M. Asiri, L. Chen, B. Tang, X. Sun, *Adv. Mater.* **2018**, 30, e1800191.
8. X. Li, T. Li, Y. Ma, Q. Wei, W. Qiu, H. Guo, X. Shi, P. Zhang, A. M. Asiri, L. Chen, B. Tang, X. Sun, *Adv. Energy Mater.* **2018**, 8, 1801357.
9. H. Huang, L. Xia, R. Cao, Z. Niu, H. Chen, Q. Liu, T. Li, X. Shi, A. M. Asiri, X. Sun, *Chem. Eur. J.* **2019**, 25, 1914-1917.
10. L. Xia, X. Wu, Y. Wang, Z. Niu, Q. Liu, T. Li, X. Shi, A. M. Asiri, X. Sun, *Small Methods* **2018**, 14, 1800251.
11. X. Wu, L. Xia, Y. Wang, W. Lu, Q. Liu, X. Shi, X. Sun, *Small* **2018**, 14, 1803111;
12. B. Xu, Z. Liu, W. Qiu, Q. Liu, X. Sun, G. Cui, Y. Wu, X. Xiong, *Electrochim. Acta* **2019**, 298, 106-111.